



Published in final edited form as:

Nanomedicine. 2011 April ; 7(2): 201–209. doi:10.1016/j.nano.2010.07.008.

Highly Stable, Ligand Clustered “Patchy” Micelle Nanocarriers for Systemic Tumor Targeting

Zhiyong Poon, Jung Ah Lee, Shenwen Huang, Richard J Prevost, and Paula T Hammond*
Department of Chemical Engineering, Massachusetts Institute of Technology, Cambridge, Massachusetts 02139, USA

Abstract

A novel linear-dendritic block copolymer has been synthesized and evaluated for targeted delivery. The use of the dendron as the micellar exterior block in this architecture allows the presentation of a relatively small quantity of ligands in clusters for enhanced targeting, thus maintaining a long circulation time of these “patchy” micelles. The polypeptide linear hydrophobic block drives formation of micelles that carry core-loaded drugs, and their unique design gives them an extremely high level of stability in vivo. We have found that these systems lead to extended time periods of increased accumulation in the tumor (up to 5 days) compared to non-targeted vehicles. We also demonstrate a 4x increase in efficacy of paclitaxel when delivered in the targeted nanoparticle systems, while significantly decreasing in vivo toxicity of the chemotherapy treatment.

Keywords

Targeted drug delivery; folate; nanoparticles

Background

Amphiphilic polymers can be designed to function as physical drug carriers in the form of micelles(1,4), permitting the entrapped drug to benefit from the enhanced material properties of the polymer nanocarrier. However, several problems still exist with micellar delivery systems. In typical carrier designs, where an anti-fouling polymer such as poly(ethylene glycol) forms the surface of the carrier, the addition of targeting ligands on the same surface nullifies the anti-fouling properties of the carrier(5-8), resulting in decreased circulation times; because of this, a key challenge to drug delivery is in the balancing of these parameters to impart the most favorable of both properties. While clinical trials of micellar delivery systems have demonstrated improved pharmacokinetics and a greater tolerance with patients, dose-limiting toxicities attributed to the drug still occurs at higher dosage levels(9-11), suggesting that on some level, the encapsulated drug dissociates from the carrier in vivo. In studies to evaluate the stability of core-loaded drugs in vivo, it was found

Corresponding author contact information: Paula T. Hammond, hammond@mit.edu, Bayer Professor and Executive Officer, Department of Chemical Engineering, Massachusetts Institute of Technology, Rm 66-352, Cambridge, MA 02139.

The authors declare no conflict of interest.

Publisher's Disclaimer: This is a PDF file of an unedited manuscript that has been accepted for publication. As a service to our customers we are providing this early version of the manuscript. The manuscript will undergo copyediting, typesetting, and review of the resulting proof before it is published in its final citable form. Please note that during the production process errors may be discovered which could affect the content, and all legal disclaimers that apply to the journal pertain.

that certain *in vivo* conditions promote the rapid release of encapsulated drugs(12), which can happen within an hour after systemic administration.

To optimize both circulation and targeting, we propose that ligand clustering, which has been shown to modulate cell adhesion and mobility on planar surfaces, can also be used as a strategy to increase tumor targeting afforded by available ligands(13,14). Through rational design, we use a block copolymer capable of highly controlled surface ligand presentation and drug loading capability by combining aspects of (i) amphiphilic linear block copolymers(15), which have the advantage of being able to entrap and protect drug in the nanocarrier core via self assembly(16), and (ii) dendrimers(17) which present polyvalent terminal units to concentrate ligands for multivalent clustered binding. This capability is particularly key to the generation of the highest affinity nanoparticle surfaces and increased specificity of intracellular uptake. The linear dendritic polymer(18) (LDP) is amphiphilic in nature, with a hydrophobic linear block independently designed to entrap drug and a hydrophilic dendritic block. An added benefit of the linear-dendritic architecture is the formation of extremely stable micelles as a result of a more effective packing of the cone-like linear-dendritic amphiphiles(18), leading to extremely low critical micelle concentrations (CMC) of order 10^{-8} mol/l, which allows the carrier to be resistant to destabilization *in vivo*. Formation of mixed micelles with non-functional dendritic blocks allows self-assembly into “patchy” ligand-clustered micelles for encapsulation of hydrophobic drugs.

Folate(19,20) has been explored in great detail for targeted cancer delivery because of the overexpression of FRs on many cancer cell types(21), particularly ovarian cancer, allowing a means for tumor selective delivery of cytotoxic drugs. In separate work, we have shown that the use of ligand-clustered micelles for folate targeting of ovarian tumor cells yields enhanced uptake both *in vitro* and *in vivo*, and that an optimum exists for cluster size and density on the patchy micellar surface ((Poon et al, *Angewandte Chemie*, 2010)). Herein, we investigate the use of these optimized novel self-assembled constructs, capable of presenting ligand in predetermined clusters on nanoparticle surfaces for cell targeting, as a means of selectively targeting drug-loaded nanocarriers for chemotherapeutics. We prepared paclitaxel PTX(22,23) encapsulated LDP “patchy” micelles that present folate in clusters and investigated the efficacy of the optimized patchy micellar system in tumor targeting, its viability as a stable drug carrier in serum and *in vivo*, as well as its efficacy for intravenous delivery of chemotherapeutics with low bioavailability.

Experimental Section

Materials

All chemicals and biologicals were purchased from Sigma-Aldrich unless otherwise noted. Paclitaxel (PTX) was purchased from LC laboratories. BALB/c mice were from Charles River, nude mice were purchased from Taconic and the folate free diet from Research Diets. All mice were fed a folate free diet for at least a week before experimentation to attain blood folate levels that are similar with humans. All *in vivo* experimentation was carried out under the supervision of the Division of Comparative Medicine (DCM), Massachusetts Institute of Technology, and in compliance with the Principles of Laboratory Animal Care of the National Institutes of Health. Cell lines were purchased from ATCC and were tested routinely for pathogens before use in animals via DCM.

Synthesis of PBLA-Polyester-PEG Linear Dendritic Polymer (LDP) and folate conjugation

The linear dendritic polymer was synthesized according to published protocols(18) with β -benzyl-L-aspartate replacing n-dodecyl-L-glutamate as the hydrophobic linear block. Folic acid was also conjugated via DCC/NHS chemistries. ($X_n = 12-15$). $^1\text{H NMR}$ (CDCl_3): δ 1.12

(m, 24H, -CH₃), δ 1.25 (m, 21H, -CH₃), δ 2.67-3.06 (bs, -COCH₂), 3.60 (d, 16H, -CH₂O), δ 4.13 (d, 16H, -CH₂O), δ 4.24-4.32 (m, 28H, -CH₂O), δ 4.56 (m, -CHNH), δ 5.03 (bs, -CH₂Ar), δ 7.22 (bs, -ArH). The steps for labeling of the polymer with radioisotopes and fluorescent dyes can be found in the supplemental information section.

Preparation of PTX loaded micelles

PTX was entrapped within both folate targeted and non-targeted LDP micelles using a nanoprecipitation method. The folate presenting micelle was self-assembled in a ratio of 2(unfunctionalized LDP): 3(20% folate functionalized LDP). A weight ratio of 10:0.25 LDP to PTX was concentrated in DMSO and mixed dropwise into PBS (at least 20X the volume of DMSO). The resultant micelles were dialyzed in a 3KMWCO dialysis bag against a PBS sink for 4h to remove the trace amount of DMSO and filtered with a 0.45 μ m teflon syringe filter before use. Additional characterization information is located in supplemental information.

Confocal analysis

KB cells overexpressing the FR receptor were cultured in FA free media on chamber slides for at least 4 days before use. PTX-AF488 conjugate (Invitrogen) was encapsulated in targeted and untargeted micelles labeled with AF647 described above. After incubation, cells were washed with PBS (2% BSA), fixed, permeabilized and stained with Hoechst before analysis with a Deltavision confocal.

In vivo experimentation

For biodistribution, a single dose of ¹¹¹In-labeled micelles (untargeted and folate targeted, 10 mg/Kg) was given via the tail vein to nude mice induced with a KB xenograft (10⁶ cells/subcutaneous injection). At predetermined time points, the mice were sacrificed and their tumors, liver, kidney, spleen, heart, lungs and blood were harvested, weighed, solubilized and radio-counted on a Beckman LS6000 scintillation counter. Animals were euthanized with CO₂ followed by cervical dislocation to confirm death. Quantitative measurements of accumulation in different tissues were normalized by the total injected dose and reported as percentage injected dose per gram tissue (%ID/g).

Toxicity of treatment was assessed in BALB/c mice (~6 months old, Charles River) given biweekly injections of various PTX containing treatments. The weight of the mice was measured regularly as an indicator of acute toxicity and blood serum was collected 4 days after the conclusion of the experiment for analysis of toxicity markers. Anti-tumor efficacy was evaluated in nude mice (3-4 weeks old, Taconic) induced with KB tumors on a single flank. Mice were randomized when the tumors were palpable (day 4) and given 4 biweekly doses of treatment (i) untargeted LDP micelles (100 mg/kg) delivering 2.5 mg/kg PX, (ii) folate targeted LDP "patchy" micelles (100 mg/kg) delivering 2.5 mg/kg PTX, (iii) 2.5 mg/kg free PTX in 1:1 Cremophor:EtOH (1 % v/v) as excipient, (iv) 10mg/kg free PTX in 1:1 Cremophor:EtOH (1% v/v) as excipient (v) LDP micelles (100 mg/kg) without PTX and (vi) Saline) on days 4, 8, 12 and 16. Throughout the trial, their weights and tumor sizes were measured once in 4 days. The length and width of the tumors were measured with calipers and the volume of the tumor was determined with the following equation: (width² X length)/ 2. Tumors that were just palpable were assigned a volume of 1 mm³. The mice were monitored for up to 60 days or until one of the following end points for euthanasia was met: 1) the body weight of the mice dropped below 15% of its initial weight, 2) the tumor burden was >2.0 cm across in any dimension, 3) the mouse became lethargic, sick or unable to feed or 4) the mouse was found dead. At the conclusion of the trial (day 60), all mice were euthanized. One-way ANOVA tests at the 95% confidence interval were used for comparison of tumor sizes.

For histology, tumors were harvested from a separate group of mice receiving the same treatment, frozen in OCT (-80 °C) and cut into 5 µm sections for analysis. Sections were fixed (5% formaldehyde) and permeabilized with cold ethanol (70% volume). TUNEL assay was performed according to the manufacturer's instructions (Molecular Probes), CD31-FITC conjugate was used to stain blood vessels and the nuclei were stained with Hoechst. Sections were examined with a Delta Vision confocal at 20X.

Results

Preparation and characterization of PTX loaded LDP micelles

The LDP has a fully biodegradable chemical composition (Figure 1A); the hydrophobic linear polypeptide block (poly(β -benzyl-L-aspartate)) forming the micelle core degrades into natural amino acids in the presence of acid and enzymes in the endosome/lysosome and the hydrophilic polyester-PEG block degrades into low molecular weight products that are readily absorbed and eliminated by the body. The apparent molecular weight was determined to be ~ 15,000 Da (polyester-PEG dendron ~ 12,000 Da; linear poly(β -benzyl-L-aspartate) ~ 3000 Da). Full synthetic details are reported separately(18). PTX was loaded in the polymeric micelles non-covalently via self-assembly of amphiphilic LDPs in aqueous milieu. During assembly, hydrophobic PTX is entrapped within the micelle core and the polyester-PEG dendron forms a dense anti-fouling shell around the micelle. Generation of the polymeric micelles was confirmed by AFM (Figure 1B). The anti-fouling shell of densely packed short PEG chains reduces non-specific uptake by non-targeted cells and prevents premature clearance of the micelles by the reticuloendothelial system (RES)(1, 3, 24). Folate-targeted micelles optimized for circulation and targeting were prepared using a mixed ratio of LDP and LDP pre-functionalized with folate on the dendron; this resulted in the formation of "patchy" micelles, on which folate is presented in clustered groupings of ~3-4 on approximately half of the micelle surface. Folate thus occupies approximately 10% of the surface (~4-5 wt% of micelle), leaving the other 90% exposed as poly(ethylene glycol).

The PTX loaded micelles have a hydrodynamic diameter of 80 ± 6 nm (mean \pm SD, n=10) with polydispersity of ~ 1.2 and a negative surface charge of -25 ± 3 mV (mean \pm SD, n=10). Addition of folate increased the hydrodynamic diameter by ~10 nm and the surface charge by ~ +5 mV. The micelles have a low critical micelle concentration (CMC) of $\sim 10^{-8}$ M. PTX can be loaded into the micellar systems with drug loading weight efficiencies up to 40 wt%, leading up to ~2 orders of magnitude increased effective solubility of PTX, but PTX-loaded micelles with 1-5 wt% PTX were found to be most stable ex vivo (Figure 1C). At low loadings, PTX is stable within the micelle core; drug release for 2.5 wt% PTX loaded micelles in serum at 37 °C and pH 7.4 were $12\pm 2\%$ and $15\pm 6\%$ at 24 h and 48 h respectively (mean \pm SD, n=3). Upon exposure to a lower pH of 5.5, PTX release from micelles is greatly enhanced (12 h: $40\pm 6\%$ and 48h: $68\pm 10\%$, mean \pm SD, n=3), indicating that a lower pH in the endosome provides a means for block copolymer breakdown, resultant micelle destabilization and drug release.

Pharmacokinetics and stability of PTX-loaded LDP micelles

Post intravenous injection in mice (n=3-5), blood plasma concentrations of the micelle carrier, encapsulated PTX (2.5 wt%) and free PTX (2.5 wt% equivalent) decreased in a two-phase log-linear fashion shown in Figure 2A and 2B. Their calculated pharmacokinetic parameters are given in Figure 2C (two compartment model(25)). The mean \pm SEM distribution half lives ($t_{1/2, \text{distribution}}$) of the LDP micelles, encapsulated PTX and free PTX were 1.83 ± 0.3 h, 1.72 ± 0.2 h, and 0.61 ± 0.4 h and their elimination half lives ($t_{1/2, \text{elimination}}$) were 15.63 ± 2 h, 9.06 ± 2 h, and 4.32 ± 3 h respectively. The similar $t_{1/2, \text{distribution}}$ but different

$t_{1/2,elimination}$ values for the LDP micelles and encapsulated PTX suggests that while encapsulated PTX was distributed within the micelle carrier for the first few hours after injection, the entrapped PTX gradually leaks out of the micelle and is cleared from the body separately as free drug. While the micelles are in systemic circulation, we believe that the main mechanism for loss of PTX is a gradual diffusion process from the micelle core, and PTX loss via micelle destabilization is kept to a minimum. Ex vivo experimental observations support this hypothesis, and show that the half-life for micelle destabilization in serum is approximately 50 h, which is much greater than the half-lives of elimination of the micelle from the body (Supplemental Figure 1). The mean \pm SEM for the rates of distribution and elimination are $K_{distribution} = 0.38\pm 0.08 \text{ h}^{-1}$ for micelles and $0.40\pm 0.07 \text{ h}^{-1}$ for encapsulated PTX; $K_{elimination} = 0.04\pm 0.02 \text{ h}^{-1}$ for micelle and $0.08\pm 0.04 \text{ h}^{-1}$ for encapsulated drug. As a small molecule drug, free PTX was distributed and cleared at a much higher rate (14x increase) compared to encapsulated PTX (mean \pm SEM: $K_{distribution} = 1.13\pm 0.3 \text{ h}^{-1}$, mean $K_{elimination} = 0.16\pm 0.2 \text{ h}^{-1}$), owing to a higher degree of extravasation into tissue and renal clearance(2); therefore, the calculated AUC value for encapsulated PTX is also higher than free PTX, indicating a much higher bioavailability of the drug if administered within the LDP micelles.

Biodistribution of micelles

The time dependent biodistribution and elimination of the LDP micelles as well as the ability of folate-functionalized micelles to target folate receptor (FR) positive KB(28,29) xenograft tumors were tested in nude mice (n = 3-5 per group, single flank tumor ~ 500 mm³). This data is shown in the form of plots of the percentage of injected dose accumulated in different organs over a period of 5 days (Figure 3A and 3B). Compared to non-tumored mice (mean \pm SEM: $37\pm 3 \text{ \%ID/g}$ at 2.5 h), blood concentration of the micelles decreased at a higher rate (3X) in tumored mice; within 3 h, micelle concentration decreased to $12\pm 4 \text{ \%ID/g}$ and $9\pm 3 \text{ \%ID/g}$ (mean \pm SEM) tissue for non-targeted and targeted micelles respectively. The faster decrease in micelle concentration in the blood is attributed to the presence of the KB tumor, which increases the rate of micelle accumulation in the tumor interstitials due to EPR. Vessel rich organs were found to contain significant levels of the micelles within 5 min after injection, and this trend is typical of a two-phase distribution and elimination pharmacokinetics. Aside from the tumors, micelle levels in all organs gradually decreased over a period of 3-5 days after injection. By day 5, most of the injected micelles were cleared from the body. The clearance patterns of micelles from the heart and lungs were similar, and no significant accumulation of micelles was observed in these vital organs. In contrast, we observed higher levels of the micelle in both the kidney and liver until day 3, indicating that urinary excretion and phagocytosis by the reticuloendothelial system (RES) are mechanisms for clearance of polymeric micelles. Most organs are also not known to express FRs(21) and therefore do not show any differences between the targeted and non-targeted micelles; however, FRs are expressed in both the kidney and liver, contributing to the accumulation of a generally higher \%ID/g level of folate-targeted micelles compared to the untargeted micelles in these organs. The expression of FR in the kidneys is limited to the apical membrane of proximal tubule cells, and thus they would only bind to folate filtered past the glomerulus(30,31); therefore, the higher \%ID/g levels in kidneys for the targeted formulation is very likely due to the retention of filtered micelles (or partially hydrolyzed LDP) via FR in the proximal tubule rather than drug containing micelles. By day 1, when most of the injected micelles were already cleared from the blood, accumulation in the kidney was $16\pm 2 \text{ \%ID/g}$ for the folate-targeted micelles and $10\pm 3 \text{ \%ID/g}$ for the untargeted micelles (mean \pm SEM).

Only the targeted micelles continuously accumulate in the tumors over a 5 day period, with the levels actually increasing for a few days before eventually decreasing (mean \pm SEM

increased from 5 ± 0.4 %ID/g at 5min to 10 ± 2 %ID/g at day 3) during a period of time when most of the non-targeted micelles were already cleared from the blood stream, a clear indicator that specific receptor mediated uptake and retention of targeted micelles was occurring. In contrast, EPR targeting of non-targeted micelles was only able to sustain high %ID/g levels for ~ 1 day; %ID/g levels in the tumor dropped from 5 ± 0.5 %ID/g to 1 ± 0.3 %ID/g between days 1 and 3. These observations are in agreement with a previous study that demonstrated longer and stronger retention of optimally targeted micelles in tumors 48 h after their administration (Poon et al, *Angewandte Chemie*, 2010). In addition to a high degree of retention, the targeted micelles were also able to extravasate within the tumor tissue (Figure 3C). We believe that the size of the LDP micelles (~80 nm in diameter) allows easy penetration of tumor tissue so that efficacy of treatment will not be hampered by inefficient delivery of chemotherapeutic agents.

Toxicity of the LDP micelles

Mice (3-5 per group) were given biweekly injections of the following: 1) LDP micelles (10 mg/kg) encapsulating PTX (2.5 wt%), 2) LDP micelles (10 mg/kg), 3) free PTX (2.5 wt% encapsulated equivalent) with 1:1 Cremophor:EtOH (1 % v/v) as excipient, 4) Cremophor:EtOH (1 % v/v) in PBS and 5) Saline for a total of 8 doses. The equivalent dose of PTX given for all injections containing PTX was 2.5 mg/kg. While no deaths occurred during the month long study, mice receiving free PTX injections lost between 10-12% of their original weight (Supplemental Figure 2) and began to show signs of hair loss after 6 injections (data not shown). Mice receiving LDP micelles with and without encapsulated PTX showed no signs of toxicity. Using an unpaired student's t-test, statistical analysis of their body weights on day 30 showed that mice receiving free PTX had statistically lower body weights ($0.0064 < P \text{ value} < 0.0157$, 95% confidence interval) than those in treatment groups 1), 2), 4) and 5). A liver panel analysis of serum collected 4 days after the conclusion of the study showed generally elevated levels of biomarkers for toxicity in mice that were receiving free PTX doses (Table 1). Similar unpaired t-tests conducted for LDP + PTX and PTX groups showed that the levels of ALK, ALT and AST ($P = 0.0013$, 0.0029 and 0.0353 respectively), as well as the weights of the spleen ($P = 0.0156$, 95% confidence interval) were statistically different.

PTX uptake and cellular trafficking

Confocal analysis of cells after 5 h of incubation with targeted micelles shows a strong overlay signal of both LDP micelle and PTX fluorescence within cytoplasmic compartments (Figure 4), indicating that the PTX-micelle conjugates are internalized (FR mediated) into endosomal compartments as whole micelles, where they can remain as a stable complex for up to 5 h. After 10 h, neither PTX nor micelle fluorescence were observed in punctuate structures within the cell; instead, diffused PTX and micelle fluorescence were found within the cytosol and the overlay signal was also significantly weaker. We believe that the low pH of 5.5 and enzymes within the endosomes trigger the release of PTX via breakdown of the polymer and destabilization of the micelle.

In our experiments, we were not able to discern a clear mechanism of PTX transfer from untargeted micelles to the cytosol; previous studies show that the uptake of hydrophobic drugs like PTX from untargeted polymeric micelles occurs via a combination of different processes(32-34): 1) PTX could be transferred from the micelles to the plasma membrane via small molecule diffusion, 2) PTX could be released in the extracellular environment for uptake by cells via pinocytosis and 3) PTX could be internalized together with the polymeric micelle via nonspecific endocytosis, with subsequent release from cellular compartments. The resulting delivery of PTX is therefore less controlled and less efficient, leading to reduced therapeutic efficiencies in vivo.

In vivo anti-tumor efficacy with KB xenografts

We evaluated the efficacy of PTX loaded LDP micelles against a KB xenograft (s.c. injection on right flank, day 0) model in nude mice. When the induced tumors were palpable, mice were randomly divided into groups of 7 for treatment (Figure 5). Compared to the controls (v and vi), all treatments showed varying degrees of efficacy in slowing the growth of the xenograft. After four doses of therapy, the mean \pm SEM (n=7) tumor sizes were 738 \pm 100 mm³, 225 \pm 45 mm³, 1230 \pm 250 mm³, 390 \pm 118 mm³, 2170 \pm 213 mm³ and 2230 \pm 159 mm³ on day 22 for treatments i, ii, iii, iv, v, and vi respectively. As seen in Figure 5A, significantly smaller tumors on PTX treatment groups were observed in comparison to control groups by ANOVA at the 95% confidence interval. Importantly, the data shows that the folate clustered micelle treatment (PTX dosage = 2.5 mg/kg) is as effective as a higher dose of free PTX (10 mg/kg), while free drug delivered at the same dose (2.5 mg/kg) had a minimal effect in slowing down tumor growth (Figure 5B). This four fold increase in therapeutic effect afforded by the targeted treatment is attributed the stronger retention of targeted micelles in tumors, as observed with biodistribution. The folate-targeted treatment had the best long-term efficacy, increasing survival time by approximately twice compared to the controls; the median survival times of the different treatment groups were 39, 48, 34, 46, 23 and 25 days for treatments i, ii, iii, iv, v, and vi respectively and the percentage mean survival time of the treated against the control (vi) (%T/C) was 158%, 201%, 138%, 186% and 100% for treatments i, ii, iii, iv, and v respectively. A mantel-cox statistical test between the survival curves show that they are significantly different with a P value of 0.001.

Untargeted micelles are not expected to be internalized by cells in significant quantity following accumulation in the tumor interstitial space; therefore, while entrapped PTX in folate targeted micelles are actively internalized by tumor cells with subsequent intracellular release of drug (Figure 4), the mechanism of PTX delivery for untargeted LDP micelles could be a combination of the different processes(33) for non-specific, random and less efficient uptake of PTX. Furthermore, biodistribution data (Figure 3) of targeted vs untargeted micelles at long time points also shows faster clearance of non-targeted LDP micelles from tumors. Histological analysis (Figure 5C) with TdT mediated dUTP nick end labeling (TUNEL) of tumors revealed the presence of apoptotic cells far away from the blood vessels. This indicates that upon arrival in the tumor, the micelles are also able to diffuse within the interstitial regions so that the delivery of PTX is not limited to tumor cells found immediately around the blood vessels, which would limit the efficacy of treatment. The body weights of the mice were monitored throughout the experiment as an indication of adverse effects of the drug. None of the mice were euthanized as a result of excessive weight loss (>15%). While all mice registered positive weight gain, those that were receiving treatments of free PTX showed smaller weight increments over the period of treatment, suggesting a low level of toxicity with the treatment (Supplemental Figure 3).

Discussion

The ability to achieve optimal ligand recognition and subsequently trigger receptor-mediated processes for endocytosis is key to the concept of targeting drugs via specific interactions. This is particularly important for cytotoxins such as cancer drugs; much larger and more regular dosages are needed to achieve therapeutic benefit if only a small percentage of the drug that reaches tumor sites are internalized. The high degree of colloidal stability of the micelles greatly enhanced the blood circulation times and bioavailability of drug. As a result, the measured circulation half-life of our encapsulated drug was significantly higher than values reported in preclinical trials for block copolymers in the literature. For example, Genexol, a poly(ethylene glycol)-*block*-poly(D,L-lactide) linear polymer carrying PTX was found to have half-lives of less than 1 h(35). The importance of drug stability within carrier systems during in vivo circulation has been given much attention lately(2,12,36). We show

that PTX is remains within the LDP carrier for at least 2 h following systemic injection, which is sufficient time to allow their distribution to tumors in significant quantity via enhanced permeation and retention(37) (EPR). Recent investigations(12,36,38) of more traditional linear block copolymers show that much of the encapsulated drug can be lost within the first 5 min after intravenous injection, leading to a different distribution profile of the drug and micelle; these observations are in contrast to our findings for the linear-dendritic systems described here. The longer stability observed can be attributed to the low micelle CMC for LDP micelles, making the system more resistant to dilution effects and destabilization by in vivo conditions; however, our data also suggests a gradual loss of PTX from the micelles at longer time points via slow leakage of drug from the interior of the micelle, and future design of the system may be applied to further address this issue.

By presentation of the folate ligand in clusters, targeting of the micelles to FR expressing cells is increased dramatically, leading to a clear observation of tumor targeting with biodistribution data indicating increased accumulation over a 5 day period. Although there have been conflicting reports(39-41) on the impact of ligand targeting on tumor biodistribution, our data supports the notion that ligands can play a meaningful role in tumor targeting after the LDP micelles are distributed to tumor sites via EPR(40,42). Both targeted and untargeted micelles accumulated similarly (~5%ID/g) via EPR in tumors after systemic administration (time points < 3 h); however, only the targeted micelles were able to efficiently enter tumor cells from the extracellular space through FR mediated uptake, leading to a higher level of retention within the tumor. Contrary to our observations, examinations of other targeted delivery systems(39-41) employing folate or a different ligand presented in a non-clustered manner on the nanoparticle surface showed that ligand targeting did not improve the biodistribution of the carrier in tumors beyond the EPR effect of non-targeted systems. We postulate that optimal cluster presentation of folate on the targeted LDP micelles enhances their avidity and increases their residence times on FR expressing KB cells in the tumor; this effect translates to a greater degree of uptake and the high level of tumor localization observed over a longer period of time is a reflection of this. This greater targeting effect also led to potency of therapy and a low PTX dose of 2.5 mg/kg given once in 4-5 days is sufficient to achieve significant anti-tumor treatment. For achieving a relatively similar effect, this dosage regimen is much lighter in comparison to other studies involving folate-mediated therapy(43-45). These studies demonstrate the use of ligand clustered linear-dendritic “patchy” micelles as an effective drug delivery system and its potential for use as a platform delivery vehicle for optimization of targeted therapy against cancers expressing other receptor targets of interest.

Supplementary Material

Refer to Web version on PubMed Central for supplementary material.

Acknowledgments

We wish to thank our funding source for this research, the National Institutes of Health (NIH) NIBIB grant R01EB008082. We thank the Koch Institute (MIT), the Institute for Soldier Nanotechnology (ISN) and the department of comparative medicine (DCM) at MIT for assistance with animal experiments and for use of facilities.

References

1. Duncan R. The dawning era of polymer therapeutics. *Nat Rev Drug Discovery*. 2003; 2:347–60.
2. Davis ME, Chen Z, Shin DM. Nanoparticle therapeutics: an emerging treatment modality for cancer. *Nat Rev Drug Discovery*. 2008; 7:771–82.
3. Allen TM, Cullis PR. Drug Delivery Systems: Entering the Mainstream. *Science (Washington, DC, U S)*. 2004; 303:1818–22.

4. Kwon GS, Okano T. Polymeric micelles as new drug carriers. *Adv Drug Delivery Rev.* 1996; 21:107–16.
5. Gu F, Zhang L, Teply BA, et al. Precise engineering of targeted nanoparticles by using self-assembled biointegrated block copolymers. *Proc Natl Acad Sci U S A.* 2008; 105:2586–91. [PubMed: 18272481]
6. McNeeley KM, Annapragada A, Bellamkonda RV. Decreased circulation time offsets increased efficacy of PEGylated nanocarriers targeting folate receptors of glioma. *Nanotechnology.* 2007; 18:385101/1–11.
7. Gabizon AA. Stealth liposomes and tumor targeting: one step further in the quest for the magic bullet. *Clin Cancer Res.* 2001; 7:223–5. [PubMed: 11234871]
8. Reddy JA, Abburi C, Hofland H, et al. Folate-targeted, cationic liposome-mediated gene transfer into disseminated peritoneal tumors. *Gene Ther.* 2002; 9:1542–50. [PubMed: 12407426]
9. Lee KS, Chung HC, Im SA, et al. Multicenter phase II trial of Genexol-PM, a Cremophor-free, polymeric micelle formulation of paclitaxel, in patients with metastatic breast cancer. *Breast Cancer Res Treat.* 2008; 108:241–50. [PubMed: 17476588]
10. Kim T-Y, Kim D-W, Chung J-Y, et al. Phase I and Pharmacokinetic Study of Genexol-PM, a Cremophor-Free, Polymeric Micelle-Formulated Paclitaxel, in Patients with Advanced Malignancies. *Clin Cancer Res.* 2004; 10:3708–16. [PubMed: 15173077]
11. Hamaguchi T, Kato K, Yasui H, et al. A phase I and pharmacokinetic study of NK105, a paclitaxel-incorporating micellar nanoparticle formulation. *Br J Cancer.* 2007; 97:170–6. [PubMed: 17595665]
12. Chen H, Kim S, He W, et al. Fast Release of Lipophilic Agents from Circulating PEG-PDLLA Micelles Revealed by in Vivo Foerster Resonance Energy Transfer Imaging. *Langmuir.* 2008; 24:5213–7. [PubMed: 18257595]
13. Biessen EAL, Noorman F, van Teijlingen ME, et al. Lysine-based cluster mannosides that inhibit ligand binding to the human mannose receptor at nanomolar concentration. *J Biol Chem.* 1996; 271:28024–30. [PubMed: 8910412]
14. Maheshwari G, Brown G, Lauffenburger DA, Wells A, Griffith LG. Cell adhesion and motility depend on nanoscale RGD clustering. *J Cell Sci.* 2000; 113:1677–86. [PubMed: 10769199]
15. Haag R, Kratz F. Polymer therapeutics: concepts and applications. *Angew Chem, Int Ed.* 2006; 45:1198–215.
16. Kataoka K, Kwon GS, Yokoyama M, Okano T, Sakurai Y. Block copolymer micelles as vehicles for drug delivery. *J Controlled Release.* 1993; 24:119–32.
17. Lee CC, MacKay JA, Frechet MJM, Szoka FC. Designing dendrimers for biological applications. *Nat Biotechnol.* 2005; 23:1517–26. [PubMed: 16333296]
18. Tian L, Hammond PT. Comb-Dendritic Block Copolymers as Tree-Shaped Macromolecular Amphiphiles for Nanoparticle Self-Assembly. *Chem Mater.* 2006; 18:3976–84.
19. Sudimack J, Lee RJ. Targeted drug delivery via the folate receptor. *Adv Drug Delivery Rev.* 2000; 41:147–62.
20. Lu Y, Sega E, Leamon CP, Low PS. Folate receptor-targeted immunotherapy of cancer: mechanism and therapeutic potential. *Adv Drug Delivery Rev.* 2004; 56:1161–76.
21. Parker N, Turk MJ, Westrick E, Lewis JD, Low PS, Leamon CP. Folate receptor expression in carcinomas and normal tissues determined by a quantitative radioligand binding assay. *Anal Biochem.* 2005; 338:284–93. [PubMed: 15745749]
22. Rowinsky EK, Donehower RC. Paclitaxel (taxol). *N Engl J Med.* 1995; 332:1004–14. [PubMed: 7885406]
23. Li C, Yu D-F, Newman RA, et al. Complete regression of well-established tumors using a novel water-soluble poly(L-glutamic acid)-paclitaxel conjugate. *Cancer Res.* 1998; 58:2404–9. [PubMed: 9622081]
24. Gref R, Minamitake Y, Peracchia MT, Trubetsky V, Torchilin V, Langer R. Biodegradable long-circulating polymer nanospheres. *Science (Washington, D C, 1883-).* 1994; 263:1600–3.
25. Rowland M, Benet LZ, Graham GG. Clearance concepts in pharmacokinetics. *J Pharmacokinet Biopharm.* 1973; 1:123–36. [PubMed: 4764426]

26. Alexis F, Pridgen E, Molnar LK, Farokhzad OC. Factors Affecting the Clearance and Biodistribution of Polymeric Nanoparticles. *Mol Pharmaceutics*. 2008; 5:505–15.
27. Yamada A, Taniguchi Y, Kawano K, Honda T, Hattori Y, Maitani Y. Design of Folate-Linked Liposomal Doxorubicin to its Antitumor Effect in Mice. *Clin Cancer Res*. 2008; 14:8161–8. [PubMed: 19088031]
28. Paulos CM, Reddy JA, Leamon CP, Turk MJ, Low PS. Ligand binding and kinetics of folate receptor recycling in vivo: Impact on receptor-mediated drug delivery. *Mol Pharmacol*. 2004; 66:1406–14. [PubMed: 15371560]
29. Reddy JA, Haneline LS, Srouf EF, Antony AC, Clapp DW, Low PS. Expression and functional characterization of the beta -isoform of the folate receptor on CD34+ cells. *Blood*. 1999; 93:3940–8. [PubMed: 10339503]
30. Salazar MDA, Ratnam M. The folate receptor: What does it promise in tissue-targeted therapeutics? *Cancer Metastasis Rev*. 2007; 26:141–52. [PubMed: 17333345]
31. Reddy JA, Allagadda VM, Leamon CP. Targeting therapeutic and imaging agents to folate receptor positive tumors. *Curr Pharm Biotechnol*. 2005; 6:131–50. [PubMed: 15853692]
32. Balasubramanian SV, Straubinger RM. Taxol-Lipid Interactions: Taxol-Dependent Effects on the Physical Properties of Model Membranes. *Biochemistry*. 1994; 33:8941–7. [PubMed: 7913831]
33. Savic R, Luo L, Eisenberg A, Maysinger D. Micellar Nanocontainers Distribute to Defined Cytoplasmic Organelles. *Science (Washington, DC, U S)*. 2003; 300:615–8.
34. Mahmud A, Lavasanifar A. The effect of block copolymer structure on the internalization of polymeric micelles by human breast cancer cells. *Colloids Surf, B*. 2005; 45:82–9.
35. Kim SC, Kim DW, Shim YH, et al. In vivo evaluation of polymeric micellar paclitaxel formulation: toxicity and efficacy. *J Controlled Release*. 2001; 72:191–202.
36. Savic R, Azzam T, Eisenberg A, Maysinger D. Assessment of the Integrity of Poly(caprolactone)-b-poly(ethylene oxide) Micelles under Biological Conditions: A Fluorogenic-Based Approach. *Langmuir*. 2006; 22:3570–8. [PubMed: 16584228]
37. Maeda H, Wu J, Sawa T, Matsumura Y, Hori K. Tumor vascular permeability and the EPR effect in macromolecular therapeutics. A review. *J Controlled Release*. 2000; 65:271–84.
38. Burt HM, Zhang X, Toleikis P, Embree L, Hunter WL. Development of copolymers of poly(DL-lactide) and methoxypolyethylene glycol as micellar carriers of paclitaxel. *Colloids Surf, B*. 1999; 16:161–71.
39. Gabizon A, Horowitz AT, Goren D, Tzemach D, Shmeeda H, Zalipsky S. In vivo fate of folate-targeted polyethylene-glycol liposomes in tumor-bearing mice. *Clin Cancer Res*. 2003; 9:6551–9. [PubMed: 14695160]
40. Kirpotin DB, Drummond DC, Shao Y, et al. Antibody Targeting of Long-Circulating Lipidic Nanoparticles Does Not Increase Tumor Localization but Does Increase Internalization in Animal Models. *Cancer Res*. 2006; 66:6732–40. [PubMed: 16818648]
41. Bartlett DW, Su H, Hildebrandt IJ, Weber WA, Davis ME. Impact of tumor-specific targeting on the biodistribution and efficacy of siRNA nanoparticles measured by multimodality in vivo imaging. *Proc Natl Acad Sci U S A*. 2007; 104:15549–54. [PubMed: 17875985]
42. Farokhzad OC, Cheng J, Teply BA, et al. Targeted nanoparticle-aptamer bioconjugates for cancer chemotherapy in vivo. *Proc Natl Acad Sci U S A*. 2006; 103:6315–20. [PubMed: 16606824]
43. Stevens PJ, Sekido M, Lee RJ. A folate receptor-targeted lipid nanoparticle formulation for a lipophilic paclitaxel prodrug. *Pharm Res*. 2004; 21:2153–7. [PubMed: 15648245]
44. Yoo HS, Park TG. Folate receptor targeted biodegradable polymeric doxorubicin micelles. *J Controlled Release*. 2004; 96:273–83.
45. Kukowska-Latallo JF, Candido KA, Cao Z, et al. Nanoparticle targeting of anticancer drug improves therapeutic response in animal model of human epithelial cancer. *Cancer Res*. 2005; 65:5317–24. [PubMed: 15958579]

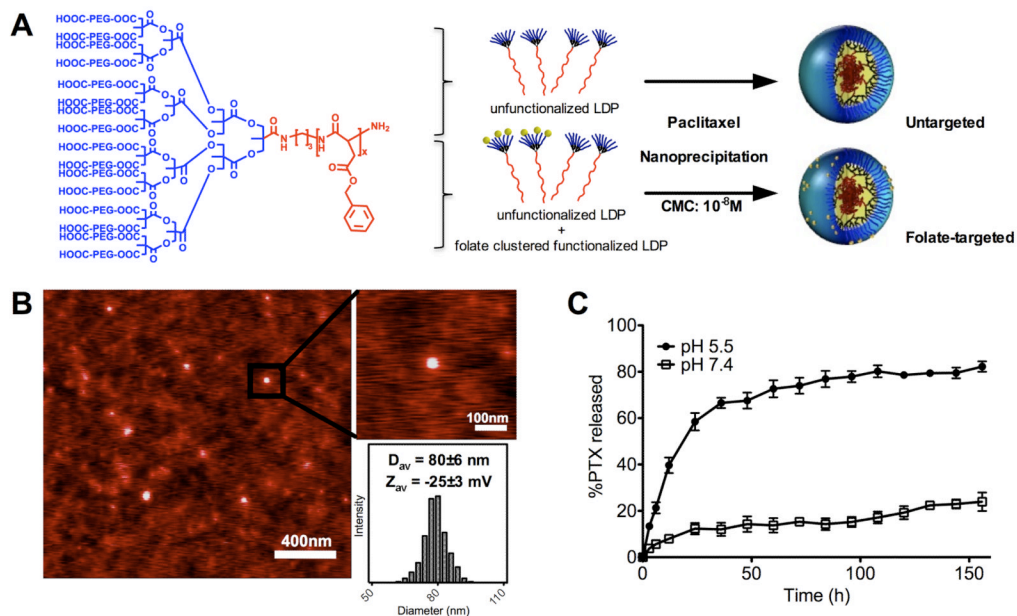
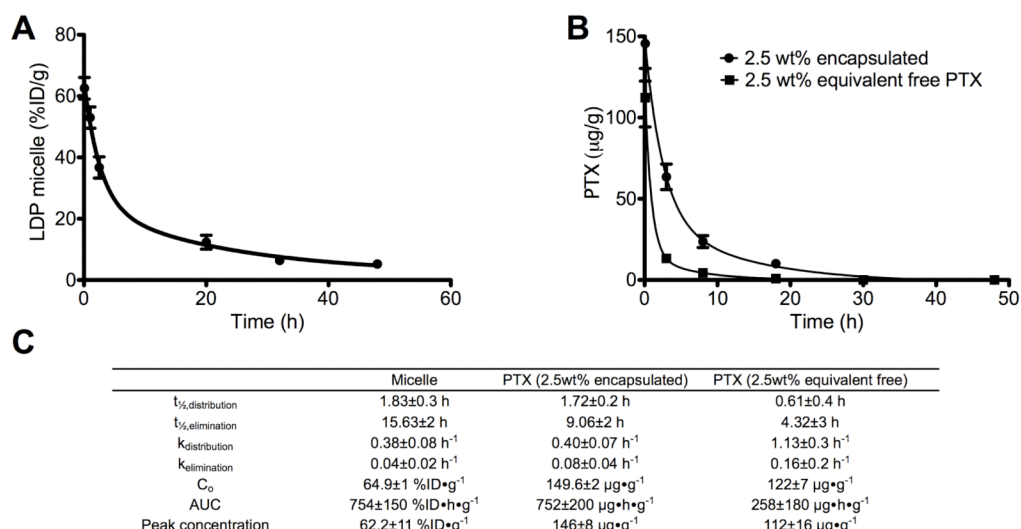


Figure 1. (A) Chemical structure of the linear dendritic polymer (LDP) made from biocompatible and degradable elements ($X_n = 12-15$). Blue = Hydrophilic, Red = Hydrophobic. Schematic showing the preparation of paclitaxel (PTX) encapsulated LDP micelles that do not present folate or present folate clusters for enhanced cell targeting. (B) Micellar morphology of PTX-untargeted LDP nanoparticles by height-mode AFM measurement. Micelle diameters are 80 ± 6 nm with a surface charge of -25 ± 3 mV by dynamic light scattering and zeta potential measurements. (C) *In vitro* release of PTX at 37°C in fetal calf serum at pH 7.4 and 5.5 shows that PTX will be stable in circulation but acidic endosomes will trigger release of PTX. (Data in mean \pm SEM)

**Figure 2.**

Blood circulation profiles of targeted micelle (A) and PTX (B) in encapsulated and free form for non-tumored BALB/c mice (mean±SEM, n=3-5). The two-phase log-linear decrease in concentration is fitted to a two compartment pharmacokinetic model: $C = Ae^{-\alpha t} + Be^{-\beta t}$. (C) Definitions: α : elimination half-life; β : distribution half-life; A: rate of loss from blood to peripheral tissue; B: rate of loss from peripheral tissue to blood; C: concentration in blood after injection; AUC, area under the curves from zero to infinity. Data is reported as percentage injected dose/gram of blood (%ID/g) for micelle and microgram of PTX/gram of blood (µg/g) for PTX.

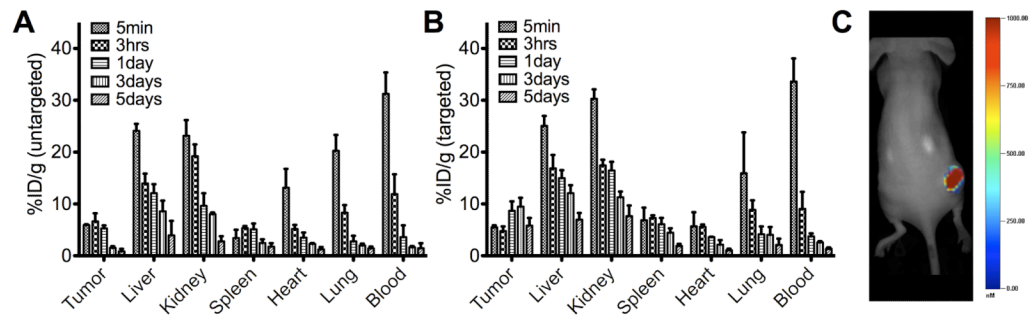


Figure 3.

Biodistribution of systemically administered LDP micelles, untargeted (A) and folate-targeted (B) in nude mice bearing KB xenografts (mean \pm SEM, n=3-5) over a 5 day period, measured in units of percentage injected dose/gram tissue (%ID/g). Slower cumulative clearance of the targeted micelle can be attributed to the sustained accumulation in KB tumors as well as the presence of FRs in the kidneys. (C) Targeted micelle imaged in the right flank KB tumor of nude mice 48 h post injection shows excellent tumor extravasation.

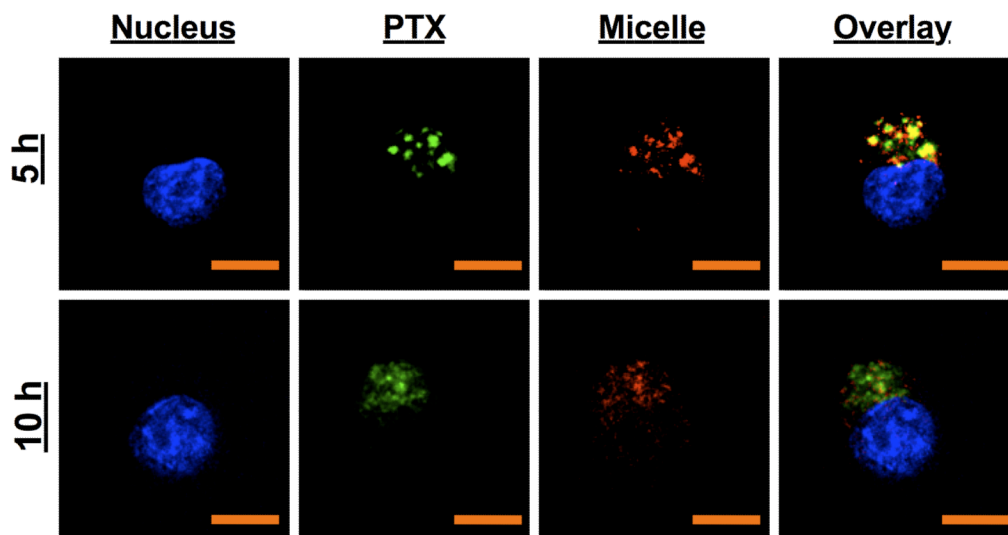
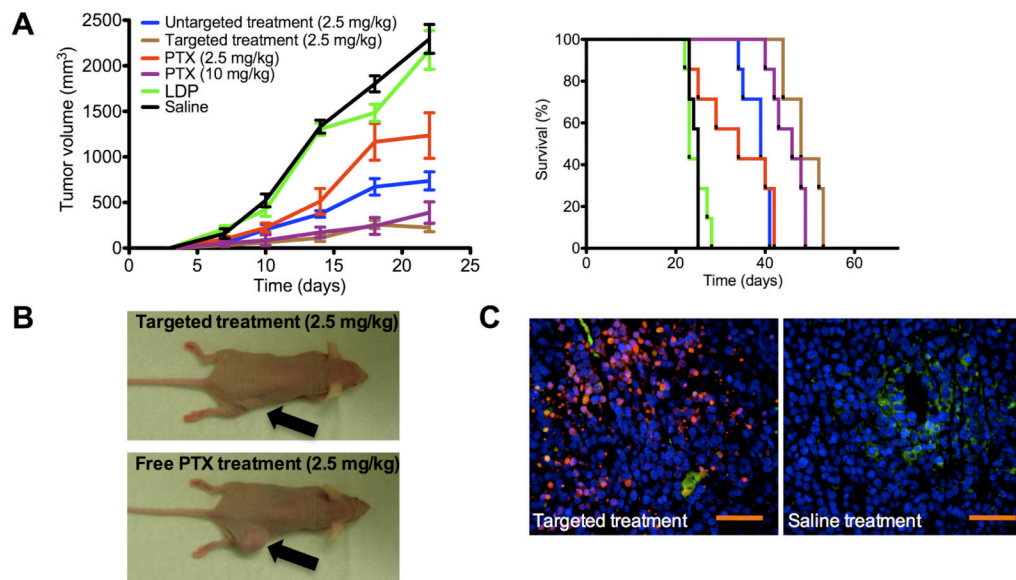


Figure 4.

Confocal microscopy analysis (60X) of the delivery of PTX (AF488, green) encapsulated in folate LDP micelles (AF647, red) in KB cells. Cell nuclei are stained with Hoechst (blue). Scale bar = 10 μ m. PTX-folate micelle conjugates are internalized as a whole via FRs and can stay within endosomes for up to 5 h. By 10 h, the low pH of 5.5 and enzymes within the endosome and lysosomes trigger the release of PTX via destabilization of the micelle and breakdown of the polymer, which then diffuses out into the cytosol to cause apoptosis.

**Figure 5.**

Anti-tumor study in nude mice ($n=7$) bearing KB xenografts (s.c. injection on right flank, day 0). Treatment began on day 4, when tumors were palpable and mice were given a single dose intravenous injection (tail vein) on day 4, 8, 12 and 16 of the following: (i) untargeted LDP micelles (100 mg/kg) delivering 2.5 mg/kg PX, (ii) folate targeted LDP micelles (100 mg/kg) delivering 2.5 mg/kg PTX, (iii) 2.5 mg/kg free PTX in 1:1 Cremophor:EtOH (1 % v/v) as excipient, (iv) 10 mg/kg free PTX in 1:1 Cremophor:EtOH (1 % v/v) as excipient (v) LDP micelles (100 mg/kg) without PTX and (vi) Saline. Mice were evaluated over a period of 60 days. A) Tumor volume over the first 22 days of treatment. Data is given in mean \pm SEM for $n=7$. Kaplan-Meier plot of survival times for mice receiving treatments also show that the targeted therapy had the best long-term efficacy. B) Representative mouse at day 20 (2 days after last treatment) for folate targeted and free PTX treatments at the same dosage level of 2.5 mg/kg. C) Representative histological sections of tumors extracted from mice receiving targeted (ii) and control (vi) treatment. Cell nuclei = blue (Hoechst); Blood vessels = green (CD31-FITC); Apoptotic cells = red (TUNEL, A647). Presence of apoptotic cells far away from blood vessels suggests that micelles were able to penetrate tumor tissue effectively. Scale bar = 250 μ m. (Data in mean \pm SEM)

Table 1

Blood chemistry of BALB/c mice (n=3-5) given biweekly i.v. injections of treatments: 1) LDP micelles (10 mg/kg) encapsulating PTX (2.5 wt%), 2) LDP micelles (10 mg/kg), 3) free PTX (2.5 wt% encapsulated equivalent) with 1:1 Cremophor:EtOH (1 %v/v) as excipient, 4) Cremophor:EtOH (1 %v/v) in PBS and 5) Saline for a total of 8 doses. Blood was taken 4 days after the final dose.

Group	ALP (U/L)	ALT (U/L)	AST (U/L)	Bilirubin (mg/dL)	Creatinine (mg/dL)	BUN (mg/dL)	Spleen (mg)
LDP + PTX	74±5	35±4	133±13	0.1±0.0	0.3±0.1	24±4	104±6
PTX	107±5	58±8	161±25	0.1±0.1	0.3±0.1	28±3	128±15
LDP	78±9	36±4	124±31	0.1±0.1	0.2±0.1	21±2	99±4
Cremophor	87±6	42±7	133±17	0.1±0.1	0.1±0.1	21±3	109±5
PBS	76±15	46±17	137±23	0.1±0.1	0.2±0.1	22±4	94±12

ALP: alkaline phosphatase; ALT: alanine aminotransferase; AST: aspartate aminotransferase; BUN: blood urea nitrogen.